Supplements

Text in supplementary material

S1 Brief overview of the ozone-prediction mode in box model

A 0-D chemical box model incorporating a condensed mechanism, the regional atmospheric chemistry mechanism version 2-Leuven isoprene mechanism (RACM2-LIM1), was used to predict ozone concentration (Stockwell et al., 1997; Griffith et al., 2013; Tan et al., 2017). In the ozone-estimation mode, the meteorological parameters, pollutants, and precursor concentrations mentioned in Section 2.2.2 were input into the model as boundary conditions, and the temporal resolution for all of the constraints was unified to 15 min. Three days of data were entered in advance as the spin-up period. The hydrogen (H_2) and methane (CH_4) concentrations were set to fixed values of 550 ppb and 1900 ppb, respectively. The physical losses of species due to processes such as deposition, convection, and advection were approximately replaced by an 18 h atmospheric lifetime, corresponding to a first-order loss rate of ~1.5 cm/s. Constraints of the observed ozone and NO concentrations were removed on the basis of the base scenario. According to the measurement accuracy, the simulation accuracy of the model for the OH and HO_2 radicals was 50% (Zhang et al., 2022). To specifically quantify the contribution of HONO-induced ozone generation, a sensitivity test was conducted without constraints on HONO (i.e., w.o HONO). Only the homogeneous reaction (OH + NO) participated in the formation of HONO in the default mode without HONO input.

Tables in supplementary material

Table.S1. Comparison of key parameters related to ozonolysis reactions (O₃、alkenes、isoprene and NOx) between YMK and the intercomparison experiment. All the values are the diurnal average (10:00-15:00).

Species	Intercomparison	YMK
O_3 (ppb)	71.02	74.58
Alkenes (ppb)	1.29	1.10
Isoprene (ppb)	0.67	0.64
NOx (ppb)	5.65	4.24

Table.S2. Detailed information of supporting measurements.

Species	Methods	limit of detection	Accuracy (1 σ)	Time resolution
OH	LIF	3.3×10^5 cm^{-3}	±13 %	60 s
HO₂	LIF	1.1×10^6 cm^{-3}	±17 %	60 s
Temperature	Met One 083E	−50 to 50 °C	±0.5 %	60 s
Relative humidity	Met One 083E	0−100 %	±2.0 %	60 s
WS	Met One 014A	0.45−60 m/s	± 0.11 m/s	60 s
WD	Met One 024A	0−360° (>0.45 m/s)	±5 °	60 s
Pressure	Met One 092	600−1100 hPa	±0.5 %	60 s
J-values	SR		± 10 %	60 s
PM₂.₅	TEOM	0.1 μg/m^3	± 10 %	60 s
O₃	UV	0.5 ppb	±10 %	60 s
NO	CL	50 ppt	±10 %	60 s
NO₂	CL	50 ppt	±10 %	60 s
SO₂	UV-F	0.1 ppb	±10 %	60 s
CO	NDIR	50 ppb	±10 %	60 s
HONO	LOPAP	10 ppt	±15 %	300 s
HCHO	Hantzsch	25 ppt	±5 %	60 s
NMHCs	GC-MS/FID	5−70 ppt	± 10−15 %	60 min

Table.S3. Photolysis frequencies for Br-related and I-related species (Atkinson et al., 2007; Bloss et al., 2010).

Reaction	Mean j(x) / j(NO₂)	References
Br₂ + $h\nu$--> Br+Br	3.45	(Atkinson et al., 2007)
BrO + $h\nu$--> Br+O	5.41	(Atkinson et al., 2007)
BrONO₂--> Br + NO₃	0.16	(Atkinson et al., 2007)
BrONO + $h\nu$--> Br + NO₂	1.14	(Atkinson et al., 2007)
BrONO + $h\nu$--> BrO + NO	1.14	(Atkinson et al., 2007)
HOBr + $h\nu$--> Br + OH	0.256	(Atkinson et al., 2007)
I₂ + $h\nu$--> I + I	20.30	(Atkinson et al., 2007)
IO+ $h\nu$--> I + O	18.30	(Bloss et al., 2001)
OIO + $h\nu$--> I + O₂	2.58	(Cox et al., 1999)
IONO₂ + $h\nu$--> I + NO₃	0.556	(Joseph et al., 2007)
I₂O₂ + $h\nu$--> IO + IO	0.556	(Joseph et al., 2007)
I₂O₃ + $h\nu$--> IO + OIO	0.556	(Joseph et al., 2007)
I₂O₄ + $h\nu$--> OIO + OIO	0.556	(Joseph et al., 2007)
INO₂ + $h\nu$--> I +NO₂	0.319	(Bloss et al., 2010)
INO + $h\nu$--> I + NO	3.71	(Bloss et al., 2010)
HOI + $h\nu$--> OH + I	1.12	(Atkinson et al., 2007)

Table.S4. Gas-phase kinetics for Br-related and I-related species in RACM2 mechanism. Revised by (Bloss et al., 2010). ACD and ACO_3 represent Acetaldehyde and Acetyl peroxy radicals, respectively, in the RACM2 mechanism. Meanwhile, MO_2 represents Methyl peroxy radicals. PI_1, PI_2, PI_3, PI_4 are the particulate iodine.

Reaction	Reaction rate constant ($cm^3 s^{-1}$)	References
$Br + O_3 \rightarrow BrO + O_2$	$1.7 \times 10^{-11}\exp(-800/T)$	(Atkinson et al., 2007)
$Br + HO_2 \rightarrow HBr + O_2$	$7.7 \times 10^{-12}\exp(-450/T)$	(Atkinson et al., 2007)
$HBr + OH \rightarrow Br + H_2O$	$6.7 \times 10^{-12}\exp(155/T)$	(Atkinson et al., 2007)
$Br_2 + OH \rightarrow HOBr + Br$	$2.0 \times 10^{-11}\exp(240/T)$	(Atkinson et al., 2007)
$Br + HCHO \rightarrow HBr + HCO$	$7.7 \times 10^{-12}\exp(-580/T)$	(Atkinson et al., 2007)
$Br + ACD \rightarrow HBr + ACO_3$	$1.8 \times 10^{-11}\exp(-460/T)$	(Atkinson et al., 2007)
$Br + NO_2 \rightarrow BrONO$	$k_0 = 4.2 \times 10^{-31}\exp(T/300)^{-2.4}$ $k_\infty = 2.7 \times 10^{-11}, F_c = 0.6$	(Bloss et al., 2010)
$BrO + BrO \rightarrow Br + Br + O_2$	2.7×10^{-12}	(Atkinson et al., 2007)
$BrO + BrO \rightarrow Br_2 + O_2$	$2.9 \times 10^{-14}\exp(840/T)$	(Atkinson et al., 2007)
$BrO + HO_2 \rightarrow HOBr + O_2$	$4.5 \times 10^{-12}\exp(500/T)$	(Atkinson et al., 2007)
$HO + HOBr \rightarrow BrO + H_2O$	5.0×10^{-11}	(Bloss et al., 2010)
$BrO + MO_2 \rightarrow HOBr + CO + H_2O$	$4.6 \times 10^{-13}\exp(798/T)$	(Enami et al., 2007)
$BrO + NO \rightarrow Br + NO_2$	$8.7 \times 10^{-12}\exp(260/T)$	(Atkinson et al., 2007)
$BrO + NO_2 \rightarrow BrONO_2$	$k_0 = 5.2 \times 10^{-31}\exp(T/300)^{-3.2}$ $k_\infty = 6.9 \times 10^{-12}\exp(T/300)^{-2.9}, F_c = 0.6$	(Bloss et al., 2010)
$BrONO_2 \rightarrow BrO + NO_2$	$2.8 \times 10^{13}\exp(12360/T)$	(Orlando and Tyndall, 1996)
$I + O_3 \rightarrow IO + O_2$	$k = 2.1 \times 10^{-11}\exp(-830/T)$	(Atkinson et al., 2007)
$I + HO_2 \rightarrow HI + O_2$	$k = 1.5 \times 10^{-11}\exp(-1090/T)$	(Atkinson et al., 2007)
$OH + HI \rightarrow I + H_2O$	$k = 1.6 \times 10^{-11}\exp(440/T)$	(Atkinson et al., 2007)
$OH + I_2 \rightarrow HOI + I$	$k = 2.1 \times 10^{-10}$	(Atkinson et al., 2007)
$NO_3 + I_2 \rightarrow I + IONO_2$	$k = 1.5 \times 10^{-12}$	(Atkinson et al., 2007)
$NO_3 + HI \rightarrow HNO_3 + I$	$k = 1.3 \times 10^{-12}\exp(-1830/T)$	(Atkinson et al., 2007)
$I + NO_2 \rightarrow INO_2$	$k_0 = 3.0 \times 10^{-31}(T/300)^{-1.0}$ $k_\infty = 6.6 \times 10^{-11}, F_c = 0.6$	(Bloss et al., 2010)
$INO_2 \rightarrow I + NO_2$	$k = 0.14\ s^{-1}$ (at 268 K)	(Bloss et al., 2010)
$INO_2 + INO_2 \rightarrow I_2 + 2NO_2$	$k = 4.7 \times 10^{-13}\exp(-1670/T)$	(Atkinson et al., 2007)
$I + NO \rightarrow INO$	$k_0 = 1.8 \times 10^{-32}(T/300)^{-1.0}$ $k_\infty = 1.7 \times 10^{-11}, F_c = 0.6$	(Bloss et al., 2010)
$INO \rightarrow I + NO$	$k = 0.087\ s^{-1}$ (at 268 K)	(Bloss et al., 2010)
$INO + INO \rightarrow I_2 + NO + NO$	$k = 8.4 \times 10^{-11}\exp(-2620/T)$	(Atkinson et al., 2007)
$IO + IO \rightarrow 2I + O_2$	$k = 0.11 \times 5.4 \times 10^{-11}\exp(180/T)$	(Atkinson et al., 2007)
$IO + IO \rightarrow I + OIO$	$k = 0.38 \times 5.4 \times 10^{-11}\exp(180/T)$	(Atkinson et al., 2007)
$IO + IO \rightarrow I_2O_2$	$k = 0.51 \times 5.4 \times 10^{-11}\exp(180/T)$	(Atkinson et al., 2007)
$IO + HO_2 \rightarrow HOI + O_2$	$k = 1.4 \times 10^{-11}\exp(540/T)$	(Atkinson et al., 2007)
$OH + HOI \rightarrow IO + H_2O$	$k = 1.0 \times 10^{-10}$	(Dillon et al., 2006)
$IO + CH_3O_2 \rightarrow CH_3O + IOO$	$k = 2.0 \times 10^{-12}$	(Dillon et al., 2006)
$IO + NO \rightarrow I + NO_2$	$k = 7.15 \times 10^{-12}\exp(300/T)$	(Atkinson et al., 2007)
$IO + NO_2 \rightarrow IONO_2$	$k_0 = 6.5 \times 10^{-31}(T/300)^{-3.5}$ $k_\infty = 7.6 \times 10^{-12}(T/300)^{-1.5}, F_c = 0.6$	(Bloss et al., 2010)
$IONO_2 \rightarrow IO + NO_2$	$k = 2.1 \times 10^{15}\exp(-13670/T)$	(Kaltsoyannis and Plane, 2008)
$IO + NO_3 \rightarrow OIO + NO_2$	$k = 9.0 \times 10^{-12}$	(Dillon et al., 2006)
$I + NO_3 \rightarrow IO + NO_2$	$k = 1.0 \times 10^{-12}$	(Dillon et al., 2006)
$IO + BrO \rightarrow I + Br + O_2$	$k = 0.2 \times 1.5 \times 10^{-11}\exp(510/T)$	(Atkinson et al., 2007)
$IO + BrO \rightarrow Br + OIO$	$k = 0.8 \times 1.5 \times 10^{-11}\exp(510/T)$	(Atkinson et al., 2007)
$IO + OIO \rightarrow I_2O_3$	$k = 5 \times 10^{-11}$	(Martin et al., 2009)
$OIO + OIO \rightarrow I_2O_4$	$k = 1.5 \times 10^{-10}$	(Martin et al., 2009)
$OIO + I_2O_3 \rightarrow PI_1$	$k = 1.5 \times 10^{-10}$	(Martin et al., 2009)
$OIO + I_2O_4 \rightarrow PI_2$	$k = 1.5 \times 10^{-10}$	(Martin et al., 2009)
$I_2O_2 + O_3 \rightarrow I_2O_3 + O_2$	$k = 1.0 \times 10^{-12}$	(Saunders and Plane, 2005)

|				
$I_2O_3 + O_3 \rightarrow I_2O_4 + O_2$		$k = 1.0 \times 10^{-12}$		(Saunders and Plane, 2005)
$I_2O_4 + O_3 \rightarrow PI_3$		$k = 1.0 \times 10^{-12}$		(Saunders and Plane, 2005)
$I_2O_2 \rightarrow IO + IO$		$k = 10.0 \text{ s}^{-1}$		(Kaltsoyannis and Plane, 2008)
$I_2O_4 \rightarrow OIO + OIO$		$k = 0.1 \text{ s}^{-1}$		(Kaltsoyannis and Plane, 2008)
$NO + OIO \rightarrow IO + NO_2$		$k = 1.1 \times 10^{-12}\exp(542/T)$		(Plane et al., 2006)
$OH + OIO \rightarrow PI_4(HIO_3)$		$k = 2.2 \times 10^{-10}\exp(243/T)$		(Plane et al., 2006)
$BrO + DMS \rightarrow Br + DMSO$		$k = 1.4 \times 10^{-14}\exp(950/T)$		(Bloss et al., 2010)
$Br + DMS \rightarrow HBr + CH_3SCH_2$		$k = 9.0 \times 10^{-11}\exp(-2390/T)$		(Bloss et al., 2010)
$IO + DMS \rightarrow I + DMSO$		$k = 1.2 \times 10^{-14}$		(Bloss et al., 2010)

Table. S5. The detailed information table for VOCs species during the YMK campaign. The mean concentration, standard deviation (SD), minimum value (Min), maximum value (Max), and percentage contribution in the species for the top-five ranked species in alkanes, alkenes, aromatic and OVOCs are listed. All the values are the daily average (0:00-24:00).

| Species	Mean (ppb)	Sd (ppb)	Min (ppb)	Max (ppb)	Proportion (%)
Alkane					
ethane	1.72	0.564	0.24	5.621	29.2
propane	1.246	0.524	0.136	5.438	21.15
n-butane	0.646	0.395	0.054	2.424	10.97
i-butane	0.561	0.471	0.029	3.372	9.52
n-hexane	0.41	0.307	0.033	3.026	6.96
Alkene					
ethene	0.592	0.656	0.034	5.48	69.08
propene	0.123	0.127	0.017	1.187	14.35
1-butene	0.046	0.014	0.012	0.107	5.37
trans-2-butene	0.028	0.006	0.006	0.05	3.27
cis-2-butene	0.026	0.006	0.007	0.045	3.03
Aromatic					
toluene	0.523	0.361	0.035	2.82	38.34
benzene	0.286	0.112	0.032	0.742	20.97
m-xylene	0.123	0.237	0.015	3.579	9.02
ethyl benzene	0.107	0.134	0.017	2.052	7.84
o-xylene	0.103	0.214	0.015	3.294	7.55
OVOC					
acetone	3.297	0.835	0.412	5.978	52.47
acetaldehyde	1.742	0.635	0.276	5.805	27.73
methyl ethyl ketone	0.496	0.15	0.051	1.118	7.89
methyl t-butyl ether	0.213	0.208	0.018	1.512	3.39
propionaldehyde	0.178	0.081	0.028	0.572	2.83

Figures in supplementary material
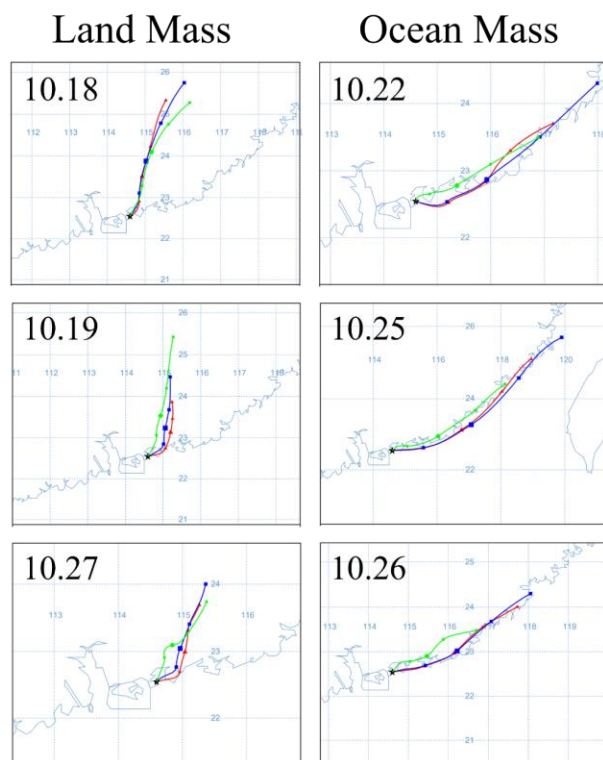
Fig. S1. The 24-h backward trajectories calculated at an arrival time of 12:00 (local time) at 100 m (red line), 500 (blue line), 1000 m (green line) above ground level at YMK in special days;
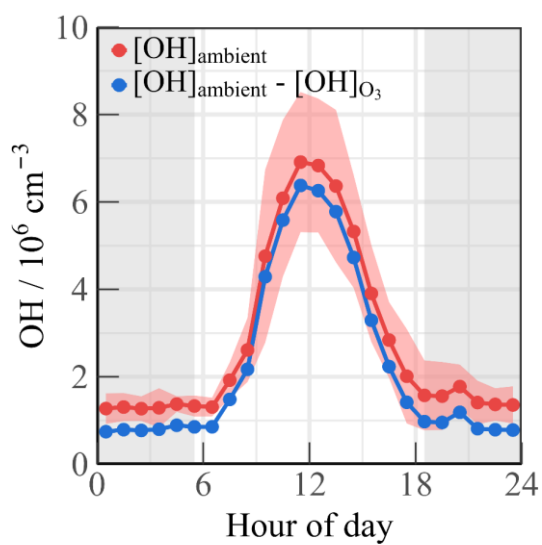

Fig. S2. Mean diurnal profiles of measured [OH] before (red line) and after (blue line) deducting the O_3 interference. The coloured shadows denote the 25 and 75% percentiles. The grey areas denote nighttime.
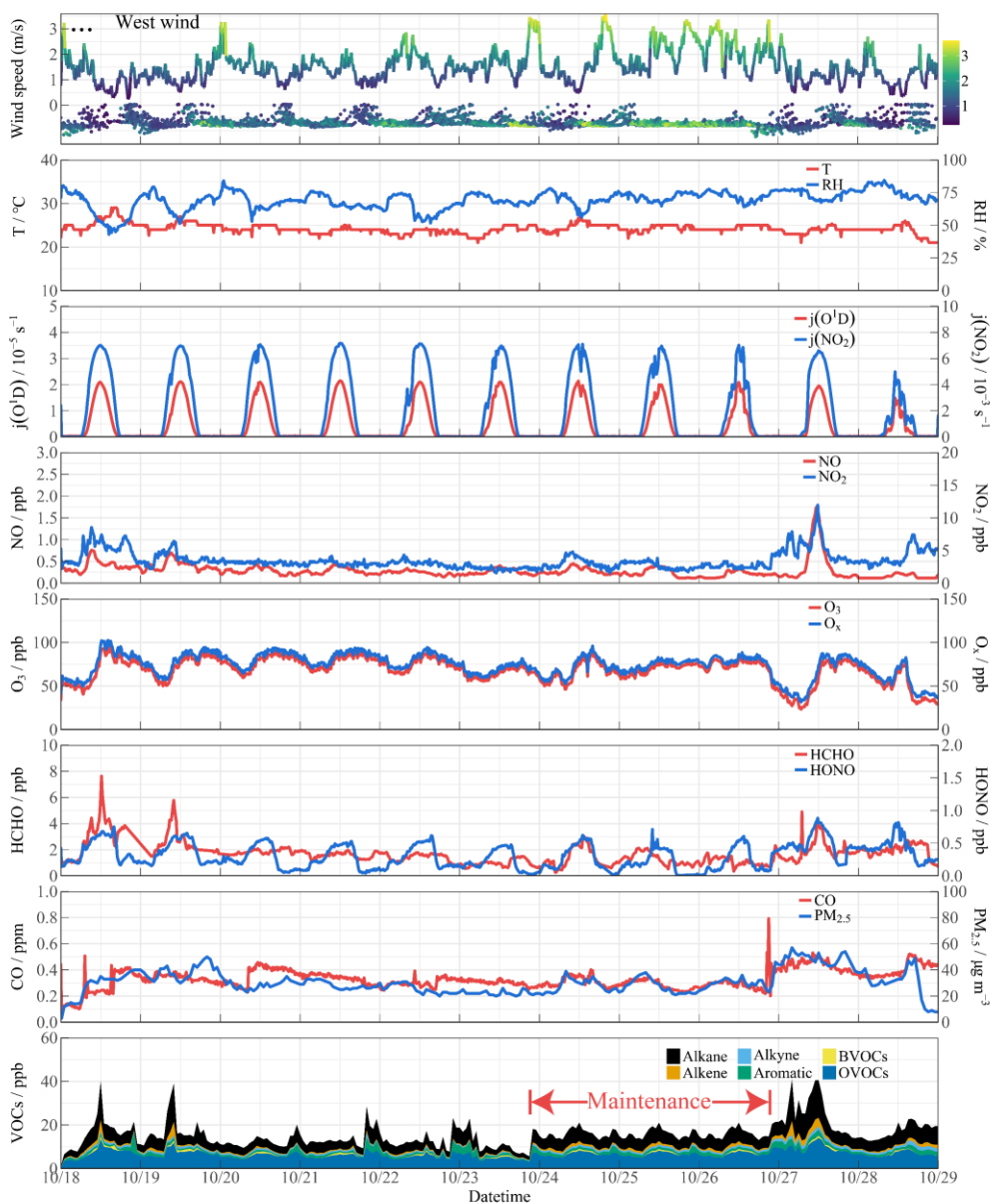
Fig. S3. Time series of observed meteorological and chemical parameters at YMK from 18 October to October 28, 2019. The GC-MS instrument failed between 24 and 26 October, and the missing VOCs data were replaced by the average value during the observation period. Only isoprene was considered in the BVOCs contribution.
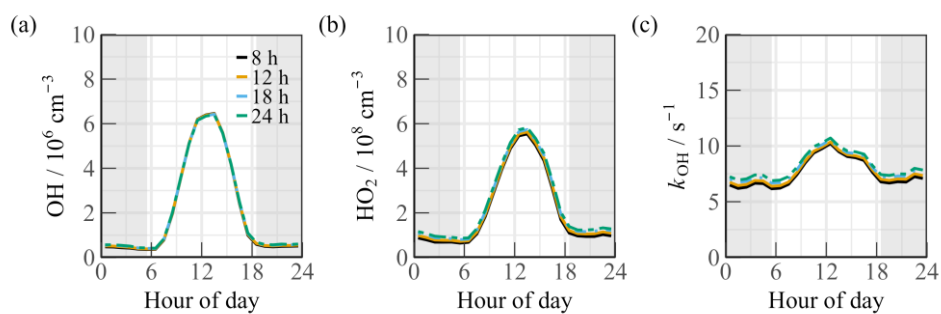

Fig. S4. The relationship between the first-order loss term and simulated **(a)** OH, **(b)** HO_2, **(c)** k_{OH} by changeing the lifetime within 8 – 24 hours (8h, 12h, 18h, and 24h).
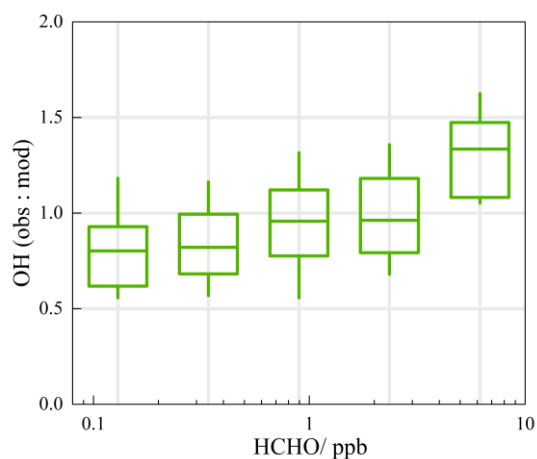
Fig. S5. The Obs-to-Mod ratio of OH radical as a function of HCHO in durinal time. Daytime data are restricted according to $j(O^1D) > 0.5 \times 10^{-5}$ s^{-1}. Boxplot gives the minimum, 25%, median, 75%, and maximum of the data.
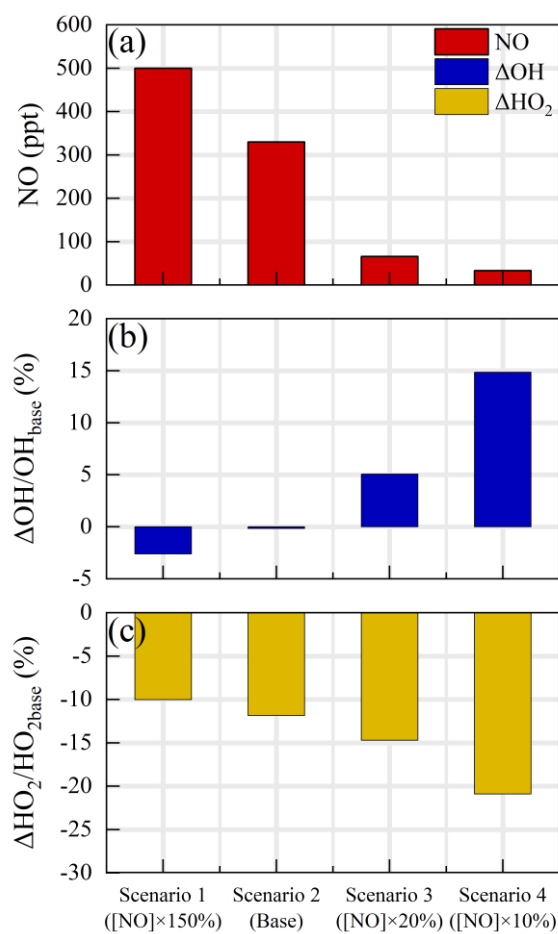
Fig. S6. By modifying the NO concentration in different levels (Scenario 1: [NO]×150%, Scenario 2: base, Scenario 3: [NO]×20%, Scenario 4: [NO]×10%), the response of HOx radicals to the halogen mechanism varied under different NO levels (30 – 500 ppt in the diurnal time).
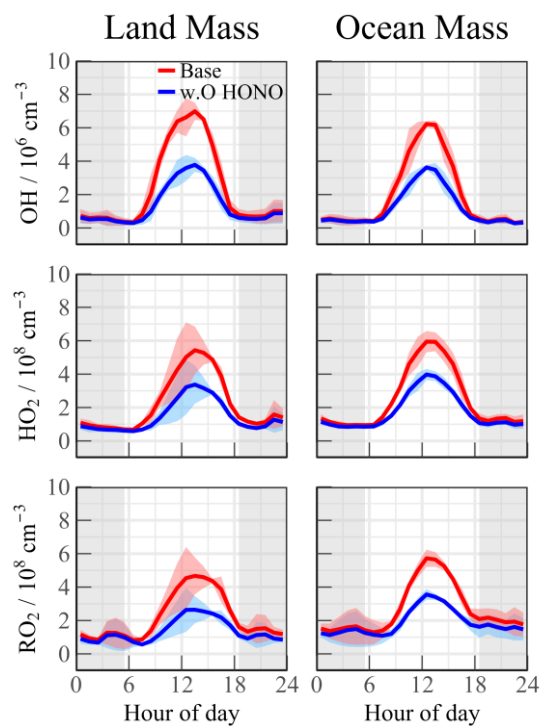
Fig. S7. The modelled OH, HO$_2$ and RO$_2$ change when the model was unconstrained to HONO during LAM and OCM sectors, respectively.

References

Atkinson, R., Baulch, D. L., Cox, R. A., Crowley, J. N., Hampson, R. F., Hynes, R. G., Jenkin, M. E., Rossi, M. J., and Troe, J.: Evaluated kinetic and photochemical data for atmospheric chemistry: Volume III - gas phase reactions of inorganic halogens, Atmos Chem Phys, 7, 981-1191, 10.5194/acp-7-981-2007, 2007.

Bloss, W. J., Rowley, D. M., Cox, R. A., and Jones, R. L.: Kinetics and products of the IO self-reaction, J Phys Chem A, 105, 7840-7854, 10.1021/jp0044936, 2001.

Bloss, W. J., Camredon, M., Lee, J. D., Heard, D. E., Plane, J. M. C., Saiz-Lopez, A., Bauguitte, S. J. B., Salmon, R. A., and Jones, A. E.: Coupling of HO<sub>x</sub>, NO<sub>x</sub> and halogen chemistry in the antarctic boundary layer, Atmos Chem Phys, 10, 10187-10209, 10.5194/acp-10-10187-2010, 2010.

Cox, R. A., Bloss, W. J., Jones, R. L., and Rowley, D. M.: OIO and the atmospheric cycle of iodine, Geophys Res Lett, 26, 1857-1860, 10.1029/1999gl900439, 1999.

Dillon, T. J., Tucceri, M. E., and Crowley, J. N.: Laser induced fluorescence studies of iodine oxide chemistry Part II. The reactions of IO with CH3O2, CF3O2 and O-3, Phys Chem Chem Phys, 8, 5185-5198, 10.1039/b611116e, 2006.

Enami, S., Yamanaka, T., Nakayama, T., Hashimoto, S., Kawasaki, M., Shallcross, D. E., Nakano, Y., and Ishiwata, T.: A gas-phase kinetic study of the reaction between bromine monoxide and methylperoxy radicals at atmospheric temperatures, J Phys Chem A, 111, 3342-3348, 10.1021/jp068390k, 2007.

Griffith, S. M., Hansen, R. F., Dusanter, S., Stevens, P. S., Alaghmand, M., Bertman, S. B., Carroll, M. A., Erickson, M., Galloway, M., Grossberg, N., Hottle, J., Hou, J., Jobson, B. T., Kammrath, A., Keutsch, F. N., Lefer, B. L., Mielke, L. H., O'Brien, A., Shepson, P. B., Thurlow, M., Wallace, W., Zhang, N., and Zhou, X. L.: OH and HO2 radical chemistry during PROPHET 2008 and CABINEX 2009-Part 1: Measurements and model comparison, Atmos Chem Phys, 13, 5403-5423, 10.5194/acp-13-5403-2013, 2013.

Joseph, D. M., Ashworth, S. H., and Plane, J. M. C.: On the photochemistry of IONO2: absorption cross section (240-370 nm) and photolysis product yields at 248 nm, Phys Chem Chem Phys, 9, 5599-5607, 10.1039/b709465e, 2007.

Kaltsoyannis, N. and Plane, J. M. C.: Quantum chemical calculations on a selection of iodine containing species (IO, OIO, INO3, (IO)(2), I2O3, I2O4 and I2O5) of importance in the atmosphere (vol 10, pg 1723, 2008), Phys Chem Chem Phys, 10, 7329-7329, 2008.

Martin, J. C. G., Ashworth, S. H., Mahajan, A. S., and Plane, J. M. C.: Photochemistry of OIO: Laboratory study and atmospheric implications, Geophys Res Lett, 36, 10.1029/2009gl037642, 2009.

Orlando, J. J. and Tyndall, G. S.: Rate coefficients for the thermal decomposition of BrONO2 and the heat of formation of BrONO2, J Phys Chem-Us, 100, 19398-19405, 10.1021/jp9620274, 1996.

Plane, J. M. C., Joseph, D. M., Allan, B. J., Ashworth, S. H., and Francisco, J. S.: An experimental and theoretical study of the reactions OIO plus NO and OH plus OH, J Phys Chem A, 110, 93-100, 10.1021/jp055364y, 2006.

Saunders, R. W. and Plane, J. M. C.: Formation pathways and composition of iodine oxide ultra-fine particles, Environmental Chemistry, 2, 299-303, 10.1071/en05079, 2005.

Stockwell, W. R., Kirchner, F., Kuhn, M., and Seefeld, S.: A new mechanism for regional atmospheric chemistry modeling, J Geophys Res-Atmos, 102, 25847-25879, 10.1029/97jd00849, 1997.

Tan, Z. F., Fuchs, H., Lu, K. D., Hofzumahaus, A., Bohn, B., Broch, S., Dong, H. B., Gomm, S., Haseler,

R., He, L. Y., Holland, F., Li, X., Liu, Y., Lu, S. H., Rohrer, F., Shao, M., Wang, B. L., Wang, M., Wu, Y. S., Zeng, L. M., Zhang, Y. S., Wahner, A., and Zhang, Y. H.: Radical chemistry at a rural site (Wangdu) in the North China Plain: observation and model calculations of OH, HO2 and RO2 radicals, Atmos Chem Phys, 17, 663-690, 10.5194/acp-17-663-2017, 2017.

Zhang, G., Hu, R., Xie, P., Lou, S., Wang, F., Wang, Y., Qin, M., Li, X., Liu, X., Wang, Y., and Liu, W.: Observation and simulation of HOx radicals in an urban area in Shanghai, China, Sci Total Environ, 810, 152275, 10.1016/j.scitotenv.2021.152275, 2022.